Acta Geodyn. Geomater.Vol.1, No.1(133), 111-119, 2004

ELECTROMAGNETIC & ACOUSTIC EMISSION FROM THE ROCK – EXPERIMENTAL MEASUREMENTS

Andrzej PRALAT and Stanislaw WÓJTOWICZ

Institute of Telecommunications and Acoustics, Wrocław University of Technology, Wybrzeże Wyspiańskiego 27, 50-370 Wrocław, Poland, Tel. +48-713202580, +48-713203118
Corresponding authors e-mail: andrzej.pralat@pwr.wroc.pl, stanislaw.wojtowicz@pwr.wroc.pl

(*Received* August 2003*, accepted* February 2004)

ABSTRACT
Measurements of electromagnetic emission (EME) from hard coal, grey dolomite, sandstone and magnesite samples subjected to a uniaxial compression are described. The measurements were performed using a system specifically designed to measure the radiation immediately preceding sample failure. The measurement results are analysed and the rocks are classified according to the potential use of their EME. The occurrence of acoustic emission (AE) in conjunction with EME as the rock sample is being loaded is analysed. Typical applications of EME to predicting hazards in the underground workings of mines are presented.

KEYWORDS: electromagnetic emission, subjecting rocks to loading, spectrum of emission

1. INTRODUCTION

The phenomenon of EME from rocks was discovered by J. Milne who at the end of the 19th century reported anomalous magnetic and electric phenomena accompanying an earthquake (Milne, 1890). Intensive research into EME from rocks has been conducted in many research centres since the early 1980s. One of the leading centres in this field is the Russian Academy of Sciences in Novosibirsk where M. Kurlenya directs research on EME from rocks. The S-diagram (fig. 1), showing changes in the frequency of EME and in spectral amplitude as the load to which a rock sample is subjected increases, is a result of this research (Kurlenya et al., 2000). At stage 1 microcracks arise in the rock. They are accompanied by high frequency EME whose frequency gradually decreases. At stage 2 crack formation begins at the reduced frequency. Branching of the cracks and the discontinuities between them lead to the appearance of higher frequencies in EME. Stage 3 is accompanied by low-frequency radiation and ends in an avalanche failure of the deformable rock sample.

The findings of the above research were practically applied to the estimation of the degree of rockburst hazard in one of the workings of the Tashtagol mine (Kurlenya et al., 2002). The anomalous EME representing the formed zone of increased rockburst hazard is recorded at distance 62.4-85 m from the face (fig. 2), which means that a stress reduction in this section is necessary.

Another centre of intensive research on EME from rocks is the Deichmann Rock Mechanics Laboratory of the Negev (Israel). V. Frid and his research team (Frid et al., 1999) register EME (emitted from a sample subjected to a uniaxial or triaxial load) using a magnetic one-loop antenna. The registered electromagnetic pulses have the shape of a decaying sine curve (Rabinovitch et al., 1999). The amplitude-frequency relation, registered for different materials, is electromagnetic field amplitude distribution inversely proportional to the signal frequency. Fractographic examinations showed (Bahat et al., 2001) that the larger the crack, the lower the EMR frequency and the higher the field intensity. The phenomena observed in the laboratory were exploited to measure EME during the infusion of water into a borehole in a rockburst-prone seam (Frid, 2000). The measuring setup consists of a loop antenna operating at a frequency of 100 kHz and a pulse counter with a set threshold for monitoring EME intensity per unit time. During the infusion of water into a bore-hole the increase in the number of fractures is accompanied by an increase in the number of pulses. With the successive injections of water the number of registered pulses decreases per unit time and so does the coal dust explosion hazard. Owing to this the injection of water can be completed.

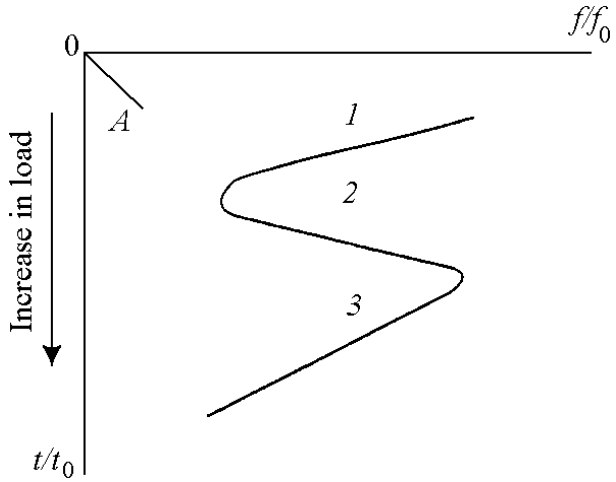

Fig. 1 S-diagram of rock failure: f/f0 – relative frequency of radiation, t/t0 – relative time, A – value of spectral amplitude; 1 – initiation and accumulation of microcracks, 2 – intergrowth and branching of cracks, 3 – avalanche failure (Kurlenya et al., 2000).

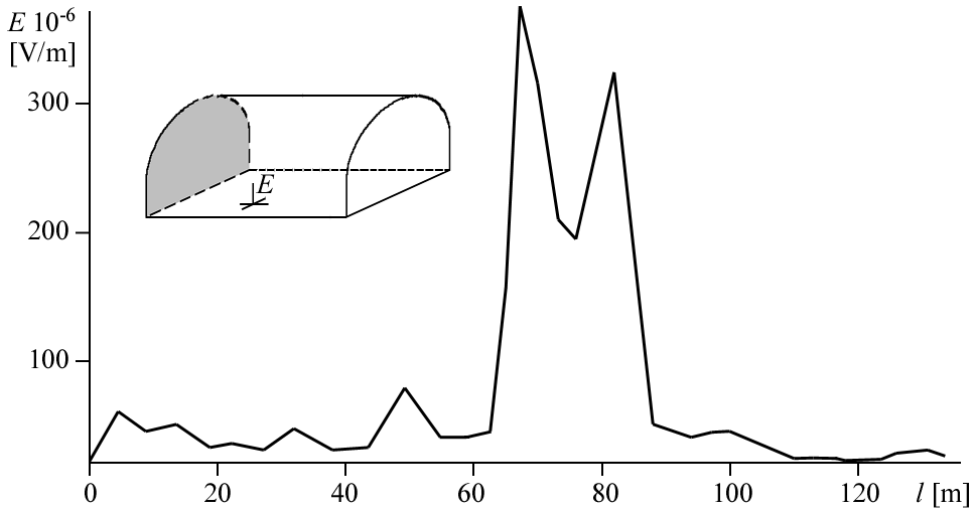

Fig. 2 Control of rockburst hazard based on EME registration (Kurlenya et al., 2002).

Research on the use of EME to monitor the level of hazard in headings has been conducted in several centres in China. This method of hazard monitoring has found probably most widespread application in this country – a special system of EME monitoring has been developed there (He et al., 2002). The system has already been applied in nearly thirty mines and the EME method of forecasting rockburst is highly valued since it does not require drilling, does not disturb work in the mine, the equipment is easy to operate and the cost of using the method is low. The system, referred to as KBD5, consists of high-sensitivity, wide frequency, directional receiving antennas, which monitor the working face. The antennas are connected to a data processing and storing device.

Fig. 3 shows a trace of EME measured at a material roadway in the working face of a mine in the course of three days, where the shifts are denoted by I, II and III (He et al., 2002). On the 17th shift I the increase in the level of EME above the critical value indicated a dangerous state. The explosion (on the 17th between shifts I and II) reduced the dangerous state, as reflected by a drop in EME. A similar situation occurred on the next day (18/II).

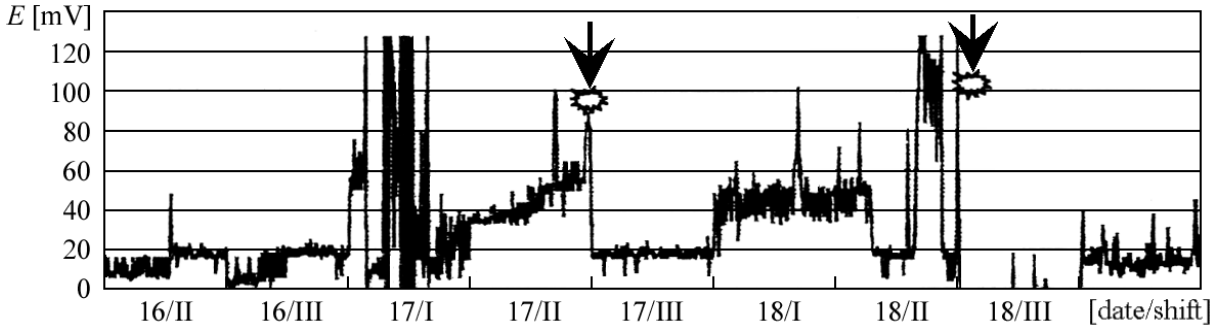

Fig. 3 Changes in EME amplitude before and after preventive measurements (He et al., 2002).

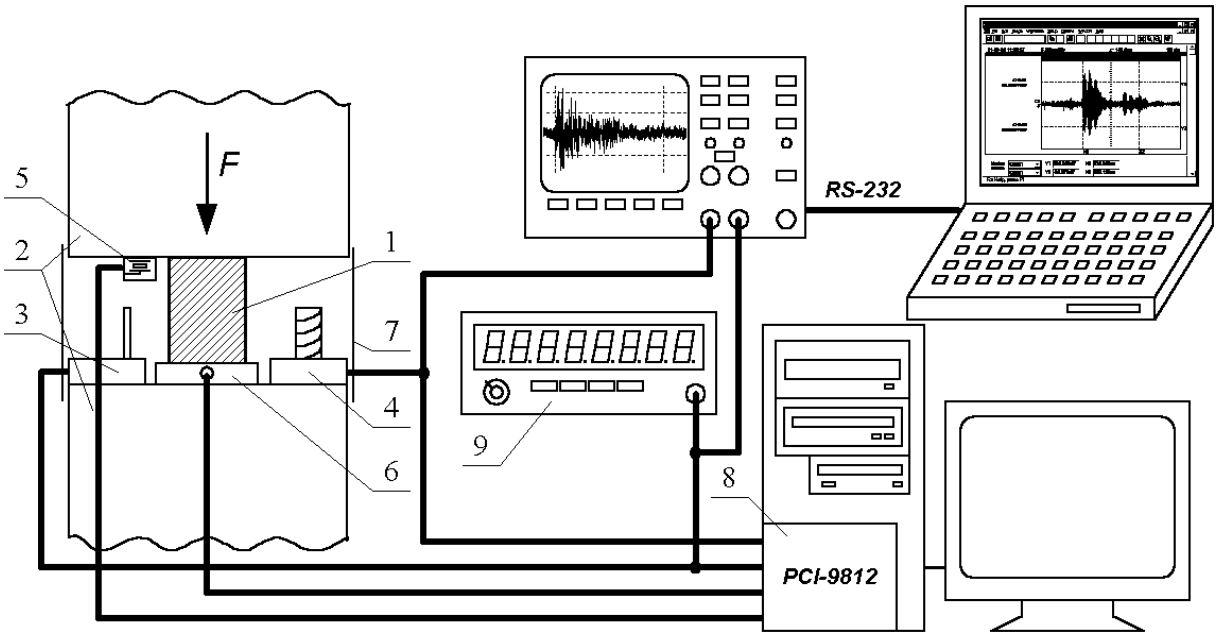

Fig. 4 Diagram of measuring system for investigating EME of rocks subjected to uniaxial stresses.

As the rock sample is subjected to a load, stresses arise in it. The stresses differ in their magnitude due to the heterogeneity of the rock's structure. As the stress in a particular part of the rock increases, free electrons are produced which generate voltage potentials. Since rock is a semiconducting medium, the electrons move from zones where stress is larger to zones where it is smaller, which amounts to a flow of current associated with magnetic field emission. As the rock fractures, the stress dynamics are high and considerable voltage differences appear which may lead to air ionisation and microdischarges.

EME from rocks shows great promise as a precursor in the prediction of hazards in the mine and so further research is needed to precisely determine the phenomenon's parameters. Therefore laboratory tests on rock samples are conducted to determine the intensity and spectrum of EME and the minimum stress at which it occurs.

2. LABORATORY STUDIES OF EME – DESCRIPTION OF MEASURING SYSTEM AND METHOD

A diagram of the measuring system used in the investigation of EME from rocks is shown in fig. 4. Tested sample (1) was mounted in stiff press plates (2). Electric field sensor (3) and magnetic field sensor (4) were placed close to the sample.

Accelerometer (5) and extensometer (6) measuring the pressure acting on the sample are fixed to the press's plate. To reduce the influence of external interfering fields on the measurement results, the whole space between the plates was enclosed within an electromagnetic shield (7).

The quantities from the four sensors were registered by a PC equipped with four-channel data acquisition card (8). The ADLINK PCI-9812 card's specifications are: up to 20M samples per second and 12-bit analog input resolution. In addition, the electric

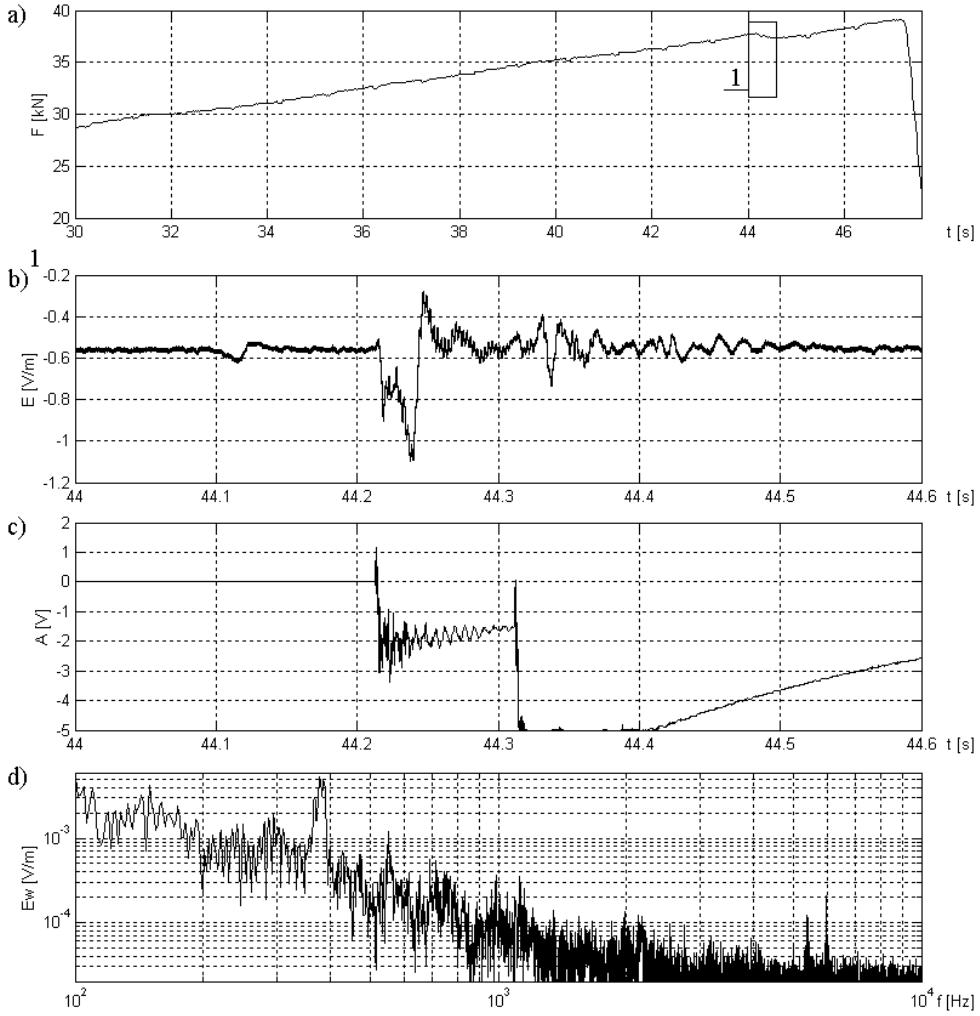

Fig. 5 Measurements of EME and AE from coal sample before failure: a – sample loading force, 1 – time interval for which measurement results are presented, b – electric field, c – AE, d – electric field spectrum.

field sensor and the magnetic field sensor are connected to the inputs of a digital oscilloscope whereby it is possible to observe traces during measurements and store them on another PC.

The setup includes pulse meter (9) for assessing the agreement between the measured magnitude of EME and the registered number of pulses. The meter is connected to the outlet of the electric field sensor.

Samples 25 mm in diameter and 50 mm high of sandstones and grey dolomites from the Lubin Copper Mine (Poland), 25×25×50 mm magnesite samples from the Lubenik Mine (Slovakia) and 35×35×60 mm hard coal samples from the Szombierki Mine (Poland) were used for the measurements.

EME was measured by two sensors: the electric sensor responding to the electric field produced by a potential difference and the magnetic sensor responding to the magnetic field generated by the passage of current. This solution was adopted because of the fact that close to the source there is no simple relationship between the electric field and the magnetic field.

The electric field sensor's antenna is a short dipole with a length of 75 mm. For the electrically short (much shorter than a wavelength) dipole the frequency characteristic is flat. The effective height of the antenna is $h_E = l/2 = 0.0375$ m, where l – the antenna's length. The gain of the amplifier, built into the sensor in order not to weight the antenna, amounts to 40 dB (high input resistance) and it is flat in a band of 100 Hz - 100 kHz (irregularity below ±0.5 dB). Since there are assembly capacitances and the amplifier's input capacitance, which form a capacitance divider, the sensor-processing coefficient measured in a field generator is 1 m. The amplifier's band is limited to 75 Hz - 120 kHz to eliminate interference and aliasing (the data acquisition card's sampling frequency is 400 kSa/s). The field sensor's antenna is put up at a distance of 50 mm from the sample subjected to a load.

The magnetic field sensor is a ferrite loop antenna with a cage coil (120 turns) and a 10×50 mm ferromagnetic core. The coil's inductance is 14.8 mH and its resonance frequency, including the assembly capacitances and the amplifier capacitance, amounts to 170 kHz. For the resonance frequency the signal is damped through the use of RC elements (a considerable reduction in the coil magnification factor). Since the effective height the loop antenna is directly proportional to frequency, an integrating amplifier (with its pole dominant at a frequency of 70 Hz) whose gain is inversely proportional to the signal frequency is employed. By combining the coil circuit with this amplifier characteristic one obtains a magnetic field sensor whose characteristic is flat in a band of 100 Hz - 100 kHz (irregularity below ±0.5 dB). Since the calculations are highly complicated, the sensor's field intensity processing coefficient was determined by placing the sensor in a uniform field generator. The coefficient is 38 Vm/A. The sensor's antenna is put up at a distance of 100 mm from the sample subjected to load.

Acoustic emission is recorded by an ENDEVCO 2219E piezoelectric accelerometer whose specifications are: resonance frequency – 20 kHz, linear processing characteristic limited to a frequency of 6 kHz, charge sensitivity – 96 pC/g, capacitance – 159 pF, processing coefficient with cable capacitance (94 pF) and charge amplifier input capacitance taken into account – 0.36 V/g, charge amplifier gain – 2.8 V/V and system's total processing coefficient – 1 V/g. The charge amplifier's gain is constant within a band up to 100 kHz. Because of the linearity of processing up to a frequency of 6 kHz, data after registration were subjected to digital low-pass filtering by limiting the accelerometer's band. Due to the considerable impulse overloads and the tendency to the generation of vibrations in the accelerometer at the resonance frequency, a charge outflow often occurs when the amplifier input voltage exceeds the supply value (the trace with a capacitance discharge time-constant). The accelerometer is fixed to the press's plate at a distance of 50 mm from the sample subjected to a load. The acoustic emission intensity is proportional to acceleration.

3. MEASUREMENT RESULTS AND THEIR DISCUSSION

From a dozen or so EME measurements four representative measurements (one for each kind of rock) were selected. The magnetic component of the EME is not included in the figures showing the traces registered prior to sample failure due to the power induction equipment (motors, transformers) level – many times stronger than the emission signal.

The figures are ordered according to the emissivity of the samples, starting from the samples whose electromagnetic emissivity is the highest and high immediately before failure and ending with the ones in the case of which no electromagnetic emissivity was observed immediately prior to failure (at fixed sensitivities of the field receivers). However, the EME registered at the moment of failure indicates that if the sensitivity of the field receivers had been increased, the traces immediately preceding sample failure could have been registered.

The largest amplitudes of EME immediately before failure were registered for the coal samples. As the coal sample was subjected to a load a few to a dozen or so impulses, whose amplitudes were many times smaller than during the failure of the sample, occurred. A fragment of the trace for the highest EME before failure is shown in figure 5. AE and EME occur simultaneously. A drop in the loading force prior to failure, accompanied by EME and AE, is characteristic of the coal samples. The electric component of the EME of the spectrum has a pulse character against the slowly changing trace. Because of its continuous character, the spectral concentration of emission shows a drop in signal amplitude with an inclination of about -30 dB/decade. Most of the energy of the EME signal is within a band of 600 Hz with a characteristic increase in the signal in a band of 370-400 Hz.

Prior to their failure the magnesite samples subjected to a uniaxial load emit an electric field whose trace includes considerably fewer slowly changing components (fig. 6). No drop in the loading force before failure, characteristic of the coal samples, occurs here and the spectrum is shifted towards higher frequencies. The signal is within a band of 1.3 kHz and the main emission bands are observed in intervals of 400-500 Hz and 610-690 Hz. AE occurred simultaneously with EME but its duration was much shorter.

Pulses were found to occur also in signals from the sandstone samples subjected to loading, but their amplitude was very small. As shown in fig. 7b, at the 27.7 second from the start of registering a pulse appeared immediately before failure, which occurred less than a second later. No AE was registered at the 27.7 second which may indicate a stronger link between stress in the sample and EME. The EME signal in the case of the electric component has a pulse character against the slowly changing trace and the duration of this component is about twice longer than the durations of the magnetic component and AE. It is clear that the magnetic component changes more slowly. The inclination of the spectral characteristics amounts to about – 30 dB/frequency decade for the two components of EME but in the case of electric emission the band is shifted towards higher frequencies.

The signal traces and the spectra for grey dolomite (fig. 8) are very similar to those for sandstone. The fact that no pulses were registered prior to sample failure may be due to the too low sensitivity of the field receivers and the considerable large amplitudes during failure indicate that EME does occur before failure.

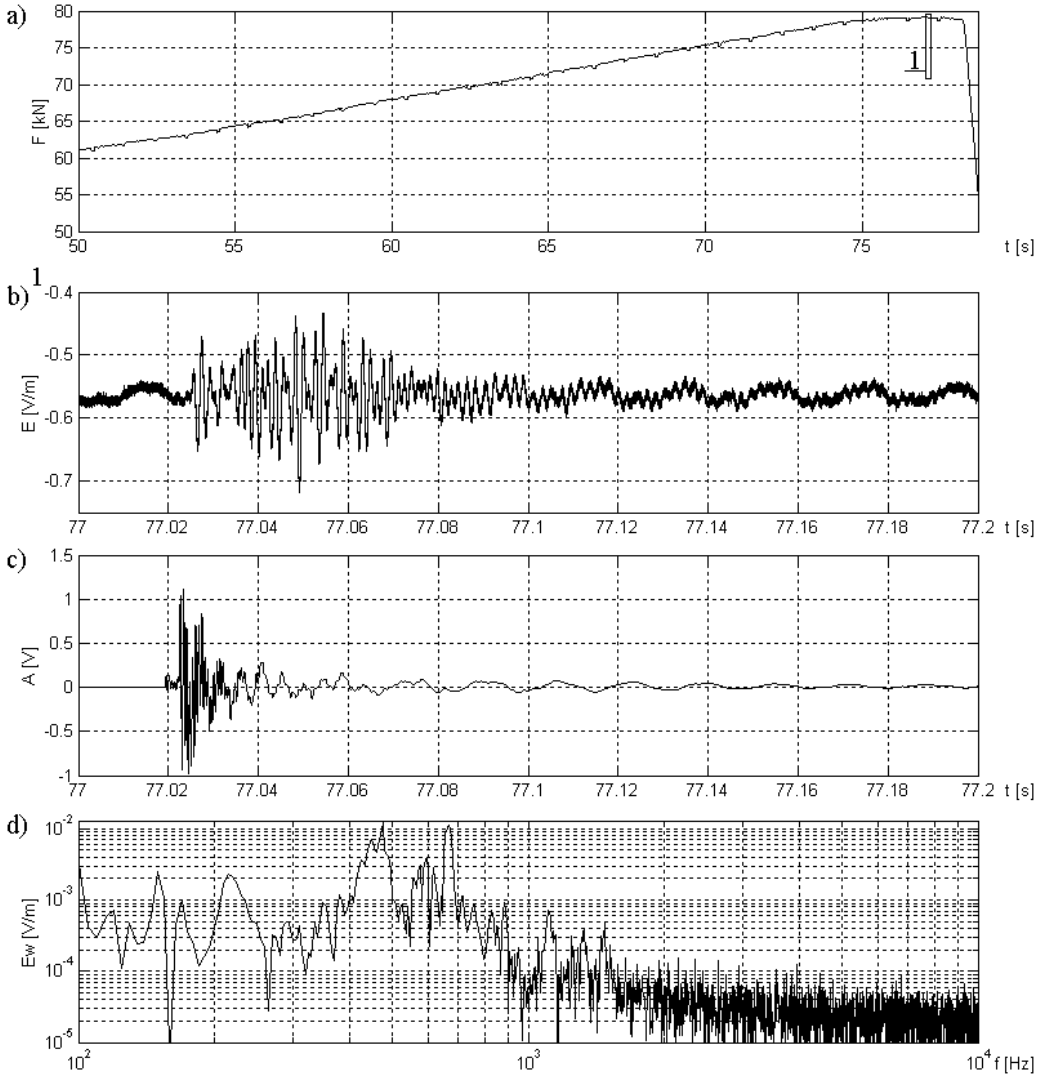

Fig. 6 Measurements of EME and AE from magnesite sample before failure: a – sample loading force, 1 – time interval for which measurement results are presented, b – electric field, c – AE, d – electric field spectrum.

4. CONCLUSION

The measurements performed on rock samples show EME to be a good precursor for determining the maximum strength of materials and suitable for determining the state of stress of the rock mass. This has been clearly demonstrated by the laboratory tests carried out on the coal samples where immediately before failure a drop in the load occurs, which is accompanied by EME and AE. An analysis of the measurement results indicates that EME more accurately reflects the state of stress of a material.

So far systems based on AE have been widely used to determine the fall hazard in mines. But the installation of such systems is time-consuming. Systems based on EME require much less time to install.

Intensive research on the application of EME to the estimation of hazards in the underground workings of mines is conducted in several centres. This research is most advanced in China where a system of monitoring based on EME has been implemented in about 30 mines and has proved to be effective.

To fully explore the possibilities of using EME for the detection of hazards in the underground workings of mines it is necessary to carry out on-site investigations to determine the level of EME proper for the interferences that occur there.

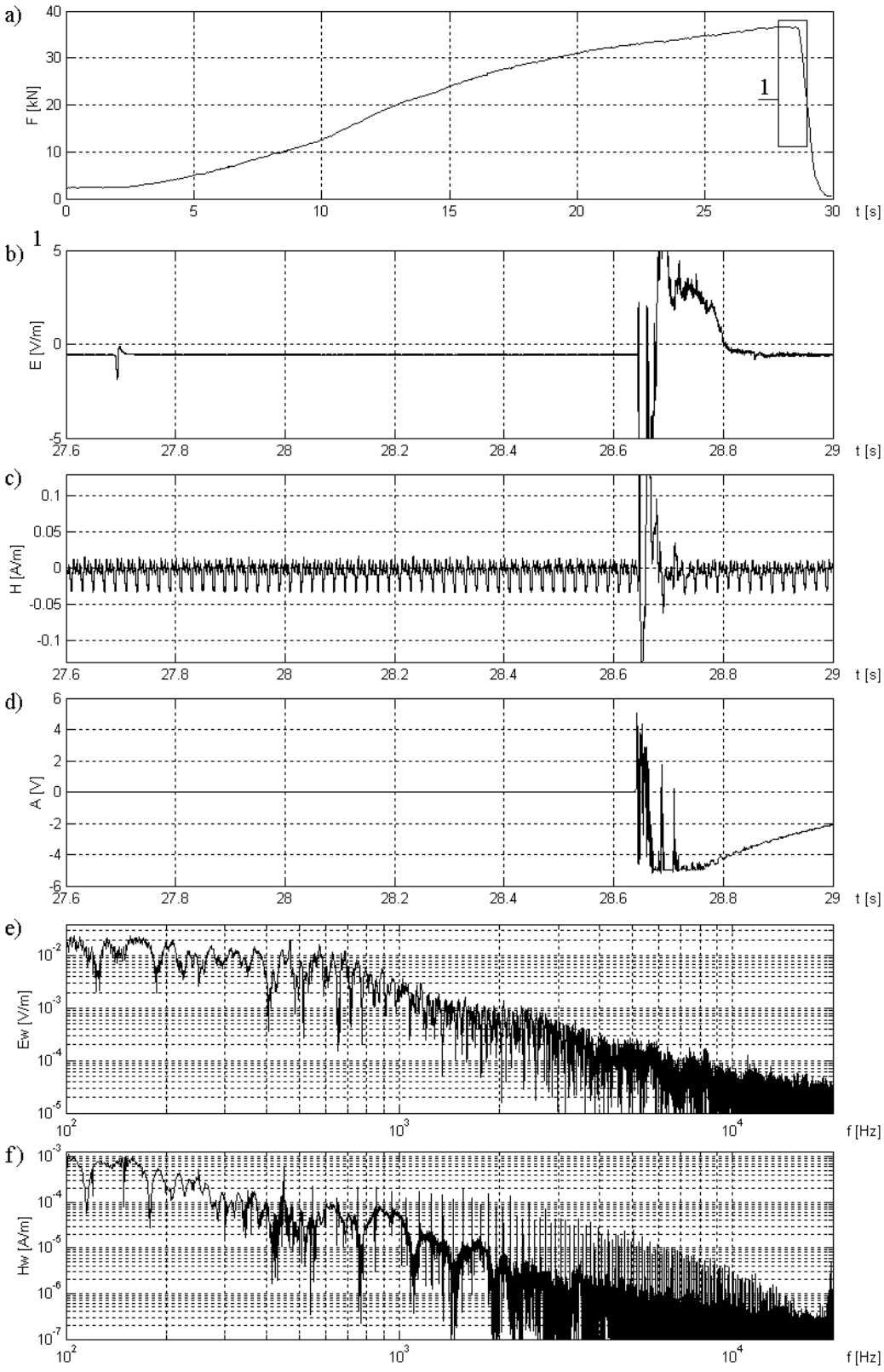

Fig. 7 Measurements of EME and AE from sandstone sample during failure: a – sample loading force, 1 – time interval for which measurement results are presented, b – electric field, c – magnetic field, d – AE, e – electric field spectrum, f – magnetic field spectrum.

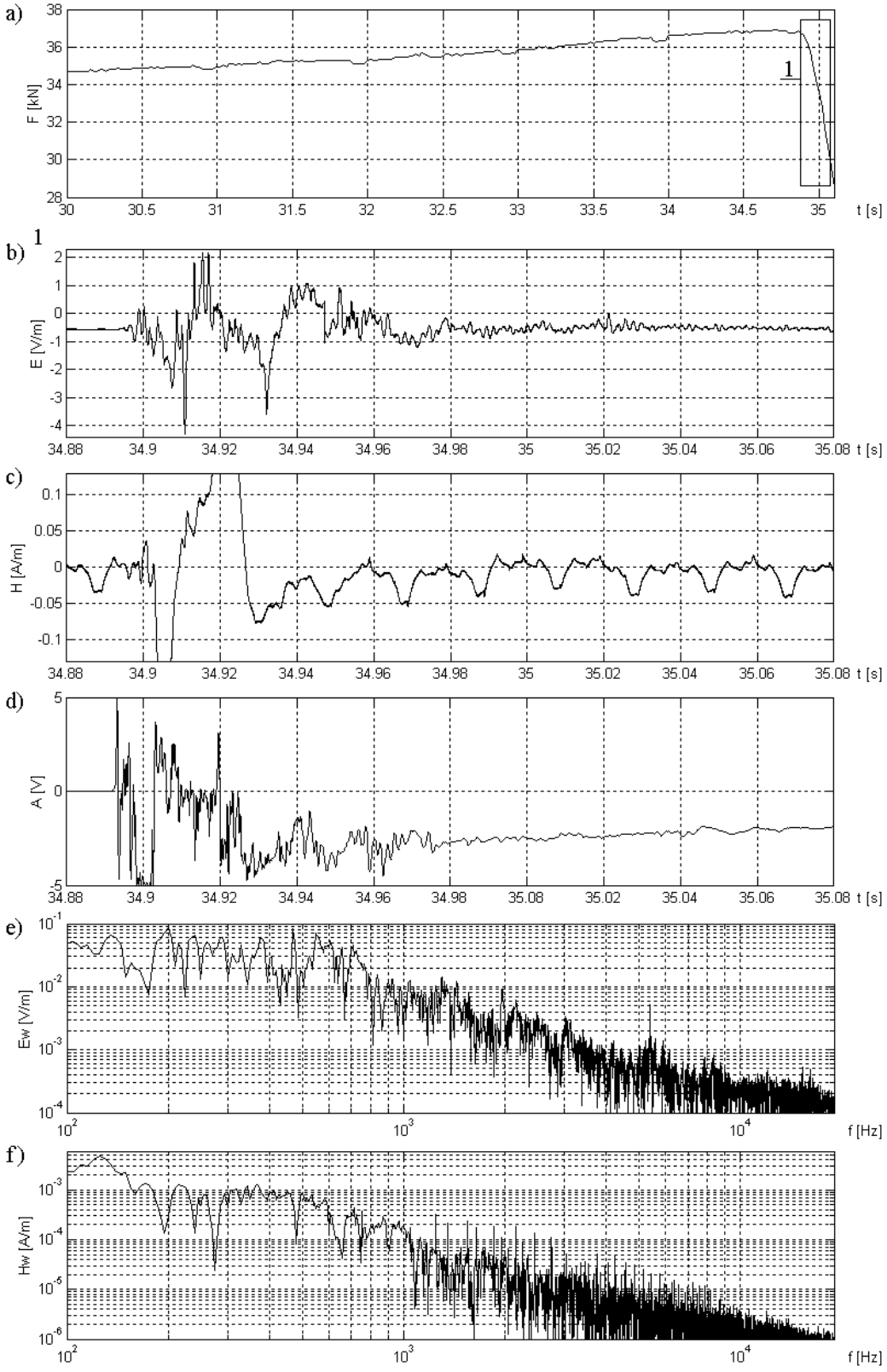

Fig. 8 Measurements of EME and AE from grey dolomite sample during failure: sample loading force, 1 – time interval for which measurement results are presented, b – electric field, c – magnetic field, d – AE, e – electric field spectrum, f – magnetic field spectrum.

REFERENCES

Bahat, D., Rabinovitch, A. and Frid, V.: 2001, Fracture characterization of chalk in uniaxial and triaxial tests by rock mechanics, fractographic and electromagnetic radiation methods. Journal of Structural Geology, 23 (10): 1531-1547 OCT.

Frid, V.: 2000, Electromagnetic radiation method water-infusion control in rockburst-prone strata. Journal of Applied Geophysics, 43 (1): 5-13 JAN.

Frid, V., Rabinovitch, A. and Bahat, D.: 1999, Electromagnetic radiation associated with induced triaxial fracture in granite. Philosophical Magazine Letters, 79 (2): 79-86 FEB.

He X., Wang E., Duo L., Nie B. and Liu Z.: 2002, Electromagnetic Radiation Monitoring System Forecasting Coal & Gas Outburst (or Rockburst) and Its Application. International Scientific-Technical Symposium Rockburst. Ustroń, Poland, 423-428.

Rabinovitch, A., Frid, V. and Bahat, D.: 1999, A note on the amplitude-frequency relation of electromagnetic radiation pulses induced by material failure. Philosophical Magazine Letters, 79 (4): 195-200 APR.

Kurlenya, M., Vostretsov, A., Kulakov, G. and Yakovitskaya, G.: 2000, Recording and Processing of Electromagnetic Emission Signals of Rock [in Russian]. Izd. Sib. Otdel.RAN, Novosibirsk.

Kurlenya, M., Vostretsov, A., Kulakov, G. and Yakovitskaya, G.: 2002, Rockburst prediction based on electromagnetic radiation of deformed rock mass. International Scientific-Technical Symposium Rockburst. Ustroń, Poland, 237-243.

Milne, J.: 1890, Earthquakes in connection with electronic and magnetic phenomena. Translations of Seismological Society of Japan, No 15, 135-162.